14-pixel, multiplexed array of gamma-ray microcalorimeters with 47 eV energy resolution at 103 keV

W. B. Doriese,[a] J. N. Ullom, J. A. Beall, W. D. Duncan, L. Ferreira, G. C. Hilton, R. D. Horansky, K. D. Irwin, J. A. B. Mates, C. D. Reintsema, L. R. Vale, Y. Xu, and B. L. Zink
National Institute of Standards and Technology, 325 Broadway, MC 817.03, Boulder, Colorado 80305

M. W. Rabin, A. S. Hoover, C. R. Rudy, and D. T. Vo
Los Alamos National Laboratory, Los Alamos, New Mexico 87545

(Received 4 March 2007; accepted 18 April 2007; published online 9 May 2007)

The authors present a prototype for a high-energy-resolution, high-count-rate, gamma-ray spectrometer intended for nuclear forensics and international nuclear safeguards. The prototype spectrometer is an array of 14 transition-edge-sensor microcalorimeters with an average energy resolution of 47 eV (full width at half maximum) at 103 keV. The resolution of the best pixel is 25 eV. A cryogenic, time-division multiplexer reads out the array. Several important topics related to microcalorimeter arrays are discussed, including cross-talk, the uniformity of detector bias conditions, fabrication of the arrays, and the multiplexed readout. The measurements and calculations demonstrate that a kilopixel array of high-resolution microcalorimeters is feasible.
 [DOI: 10.1063/1.2738371]

Gamma-ray spectrometry is an important technique in the nondestructive assay of nuclear materials. The state-of-the-art spectrometer is the high-purity, planar Ge detector, which has a collecting area of ≈ 2 cm^2, a photon count rate of ≈ 50 kc/s, and energy resolution of about 500 eV [full width at half maximum (FWHM)] when measuring 100 keV photons. Recently, several groups have demonstrated microcalorimeter spectrometers with sub-100-eV energy resolution at 100 keV,[1–3] which will allow line separation in the complicated Pu γ-ray spectrum. Because individual γ-ray microcalorimeters are relatively small (≈ 1 mm^2) and slow (50–100 c/s), a fieldable instrument will require an array of microcalorimeters to increase the collecting area and count rate. In this letter, we present a prototype, 14-pixel, multiplexed array of transition-edge-sensor (TES) microcalorimeters. All aspects of our array architecture, including fabrication and assembly, cryogenics, and the multiplexed readout, are compatible with kilopixel-scale arrays.

A TES microcalorimeter uses a thin film, electrically biased in its superconducting-to-normal-metal transition, as a sensitive thermometer. Deposited heat from an absorbed photon increases the temperature and resistance of the film. The resulting pulse-shaped decrease in the device current is used to measure the energy of the photon.

The TES microcalorimeters described in this letter are similar to the single detector presented by our group.[3] Each TES is a 400 μm square thin-film bilayer of Mo and Cu, with a superconducting transition temperature tuned to $T_c \approx 100$ mK and a normal-state resistance of $R_n \approx 8$ mΩ. Cu bars abate "unexplained noise"[4] and tune the transition width.[5] A 6.25 mm chip contains a 4×4 array of detectors on a 1.3 mm pitch (see Fig. 1). In order to stop the γ rays, a bulk, polycrystalline-Sn absorber (900 μm square $\times$ 250 μm thick) is glued to a lithographically patterned epoxy post on each detector. The calculated quantum efficiency of the absorbers is about 25% for 100 keV photons. The entire detector plane, pictured in Fig. 1, is cooled to 50 mK by an adiabatic-demagnetization refrigerator (ADR).

Single TES microcalorimeters are read out by multistage, superconducting-quantum-interference-device (SQUID) amplifiers, which are well matched to the low output impedance and low current noise of TESs. For large arrays of TESs, the complexity and heat load due to having a complete SQUID amplifier channel for each detector have motivated the development of multiplexing schemes.[6,7]

The 14-pixel array was read out with two SQUID amplifier columns using a cryogenic time-division multiplexer (TDM) (see Fig. 2). The 8-row $\times$ 2-column TDM had two unused rows in column 2. Because the TDM architecture[8,9] was developed for arrays of high-speed (sub-100-μs) x-ray

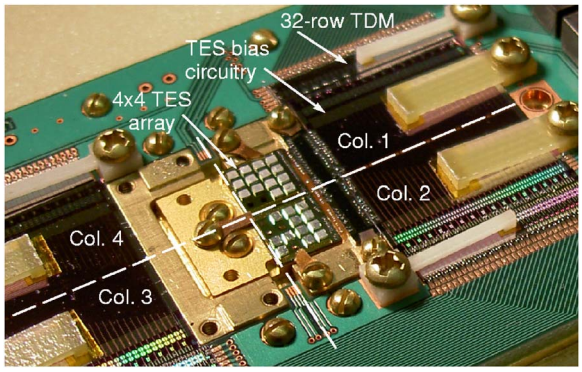

FIG. 1. (Color online) Two 4×4-pixel detector array chips and supporting cryogenic electronics. To build each array chip, the Sn absorbers were assembled into a micromachined caddy, and then all 16 were glued to the array at once. Of the 32 possible detectors on the two chips, 18 failed for various reasons, which have since been addressed; subsequent array assemblies have yielded absorbers on all pixels. The remaining 14 detectors survived repeated thermal cycling between cryogenic and room temperatures, and were used for the experiments described in this letter. We anticipate being able to assemble single-chip arrays of up to about 100 pixels; these arrays would then be tiled to reach the kilopixel scale. The interface-wiring and SQUID-TDM chips shown here contain circuitry to read out 128 detectors through four amplifier columns.

[a]Electronic mail: doriese@boulder.nist.gov

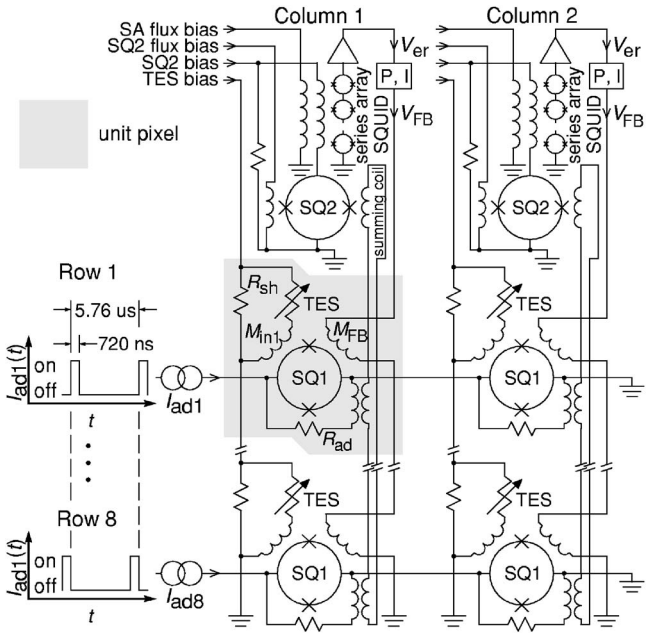

FIG. 2. Schematic of the 2-column×8-row SQUID-time-division multiplexer. Each TES is inductively coupled (M_{in1}) to its own first-stage SQUID amplifier (SQ1). An inductive summing coil carries the output signals from all SQ1's in a column to a common second-stage SQUID (SQ2). Rows of SQ1s are sequentially turned on using I_{ad}, so the signal from one TES at a time per column is passed to that column's SQ2 (there need not be any relation between rows/columns in the TES array and in the TDM). Finally, the output of each SQ2 is routed to a 100-SQUID, series-array amplifier and then to room-temperature electronics. In order to keep the nonlinear three-stage SQUID amplifier in a small, linear range, the multiplexer is run as a flux-locked loop. The series array output, or error signal (V_{er}), is digitally sampled, and then a flux-feedback signal (V_{FB}) is applied inductively to the first-stage SQUIDs to servo V_{er} to a constant value. A linear combination of V_{FB} and V_{er} gives the TES current. Electronics synchronize the row-address and flux-feedback signals and stream the data to a computer.

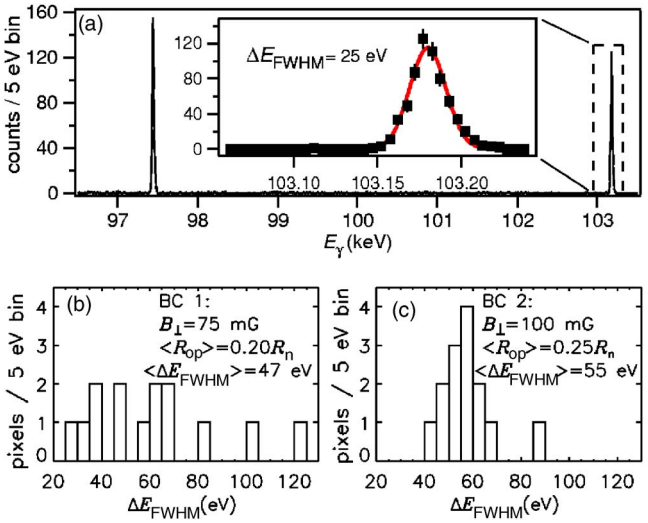

FIG. 3. (Color online) Spectral energy resolution. (a) The best performance of a single detector, ΔE_{FWHM}=25 eV at 103 keV, was achieved under BC 1. This performance was repeatable over months and was achieved when the detector was read out both through the 2×8 TDM and in single-detector mode. [(b) and (c)] Histograms of ΔE_{FWHM} for the 14 pixels under BCs 1 and 2.

microcalorimeters,[10] the readout of 14 relatively slow γ-ray TESs, which had an average pulse-decay time constant of 2 ms, was not difficult. The performance of the detectors was not measurably degraded by the multiplexed readout. We calculate, based on the previous work,[10] that the TDM system would require an open-loop bandwidth of $f_{OL} \geqslant 2$ MHz and nonmultiplexed amplifier noise (referred to the first-stage SQUID) of $N_{SQ1} \leqslant 0.3\ \mu\Phi_0/\sqrt{\text{Hz}}$ in order to read out a 32-row×32-column array of 25 eV resolution γ-ray microcalorimeters with a resolution degradation of no more than 5%. The prototype TDM system used here, which was not near the calculated performance limits, approached these requirements, with f_{OL}=1.6 MHz and N_{SQ1}=0.47 $\mu\Phi_0/\sqrt{\text{Hz}}$.

To measure its spectrometric performance, the 14-pixel array was illuminated by a ^{153}Gd γ-ray source. The count rate recorded by each detector was 7 c/s. After pileup events were removed, pulses due to γ rays were optimally filtered.[11] The resulting pulse-height spectrum from each detector was spline corrected to remove gain drifts over time and then converted to energy units by use of a linear fit to the known 97.43 and 103.18 keV γ-ray lines. Through the rest of this letter, we quote the energy resolution of a detector, ΔE_{FWHM}, as measured from the 103 keV line.

The design value of the heat capacity C of a TES microcalorimeter[5] strikes a delicate balance between keeping the saturation energy, $E_{sat} \propto C$, higher than the spectral energies of interest and not degrading the energy resolution, $\Delta E_{FWHM} \propto \sqrt{C}$. Complicating matters, the average T_c of an array of TESs, on which the operating T and thus C strongly depend, is sometimes difficult to control due to variations in the bilayer interface conductance.[12] While experiments have shown that the average T_c of TESs on a production wafer can be tightly controlled, methods to operate arrays made with a nonoptimal average T_c (and thus, C) are desirable. We describe such a method, which involves an applied magnetic field.

The average critical temperature of the 14 TESs was $\langle T_c \rangle$=94 mK, which was below the target value of 115 mK. The phonon-dominated C of the superconducting Sn absorbers ($C_{Sn} \propto T^3$) was thus about half the design value, with the result that the response to 100 keV photons was highly nonlinear. To increase the dynamic range of the detectors, a magnetic field, $B_\perp \approx 100$ mG, was trapped in the Sn absorbers as they were cooled through their superconducting transitions (≈3.8 K) during the ADR cycle. The field broadened the R vs T transitions of the TESs.[4]

We present results for two combinations of $\langle R_{op} \rangle$, the average quiescent resistance of the detectors under common bias, and $B_\perp$. Bias condition (BC) 1 ($B_\perp$=75 mG and $\langle R_{op} \rangle = 0.20 R_n$) was selected to optimize the performance of a single pixel, which achieved ΔE_{FWHM}=25 eV [see Fig. 3(a)]. The best previously published resolution for a γ-ray microcalorimeter was 42 eV at 103 keV.[3] The ΔE_{FWHM} of all detectors were scattered from 25 eV to 124 eV [see Fig. 3(b)]. BC 2 ($B_\perp$=100 mG and $\langle R_{op} \rangle = 0.25 R_n$) was chosen to minimize the variation in ΔE_{FWHM}. Here, all but one of the detectors had ΔE_{FWHM} between 40 and 70 eV [see Fig. 3(c)].

The effective energy resolution of an inhomogeneous array of detectors depends on what measurement is being performed with the array. For many common spectral measurements, such as line positions or peak areas above background, the measurement from each pixel would be weighted by the inverse square of its energy resolution and by the number of counts in its spectrum. Assuming equal counts per pixel, the weighted-average energy resolution of

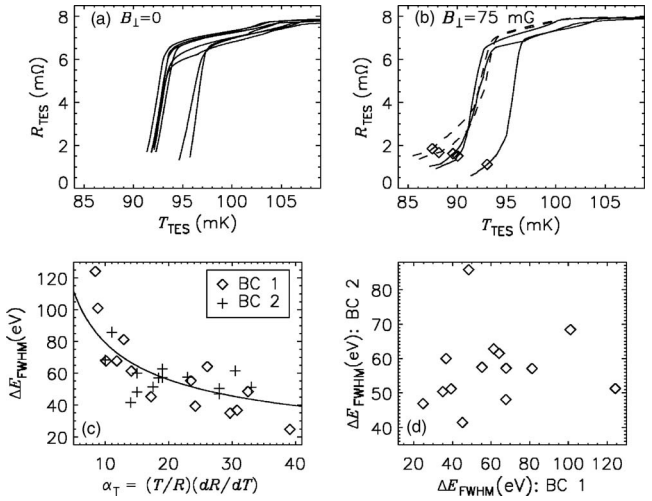

FIG. 4. Pixel uniformity. (a) R vs T transitions for the eight pixels in column 1, in $B_\perp=0$ (the six pixels from column 2 are omitted for clarity). The transition shapes are highly uniform in the 2–6 mΩ range: at 2 mΩ, all 14 pixels have slopes in the range $94 \leqslant \alpha_T \leqslant 105$, with $\langle \alpha_T \rangle = 101$. When a photon event drives R_{TES} above the sharp bend at 6–7 mΩ, the TES saturates and shows a highly nonlinear response. (b) R vs T transitions for the two worst (dashed) and three best (solid) pixels in $B_\perp=75$ mG. The field broadens the transitions to allow sufficient dynamic range at $\langle R_{op} \rangle = 0.20 R_n$ (BC 1; the quiescent bias points are shown as diamonds), at the expense of nonuniform kinking low in the transitions. (c) Energy resolution vs α_T (measured at the quiescent operating point) for all 14 pixels, under BCs 1 and 2. The solid curve shows the generally accepted microcalorimeter prediction, $\Delta E_{FWHM} \propto 1/\sqrt{\alpha_T}$, with an arbitrarily selected constant of proportionality. (d) The energy resolution of each detector under BC 2 vs under BC 1. The performances under the two bias conditions have a linear correlation coefficient of $r=0.14$.

the array in making such a measurement would be

$$\langle \Delta E_{FWHM} \rangle = \left(\frac{1}{N} \sum_{i=1}^{N} \frac{1}{(\Delta E_i)^2} \right)^{-1/2}. \quad (1)$$

Under BC 1, the 14-pixel array achieved $\langle \Delta E_{FWHM} \rangle = 47$ eV at 103 keV, meaning that a measurement made with the array would attain the same statistical significance per unit time as would one made with a 14-pixel array of identical, 47 eV resolution detectors. The best previously reported microcalorimeter-array result in this energy range was two pixels with 64 eV resolution at 60 keV.[1]

Although it does linearize the detector responses, the addition of $B_\perp$ brings about variations in the shapes of the superconducting transitions, whose causes we are still investigating. These variations cause the large spread in performance of the 14 otherwise similar pixels, and account for the difference between the wide scattering of ΔE_{FWHM} under BC 1 and the tighter grouping under BC 2. In $B_\perp=0$, the transition shapes are very smooth and uniform [see Fig. 4(a)]. However, in $B_\perp=75$ mG, kinks appear low in the transitions, resulting in widely scattered values of the transition slope, $\alpha_T=(T/R)(dR/dT)$, at the optimal quiescent bias point of $\langle R_{op} \rangle = 0.20 R_n$ [BC 1, see Fig. 4(b)]. In $B_\perp=100$ mG the transitions (not pictured) look generally similar to the 75 mG case, but are broadened just enough to allow a quiescent bias point, ($\langle R_{op} \rangle = 0.25 R_n$, or BC 2), which is above the worst of the kinks. Figure 4(c) shows the correlation between ΔE_{FWHM} and α_T. Figure 4(d) provides evidence that the pixels are not inherently different from one another, as their performances under BCs 1 and 2 are weakly correlated. In future arrays, we will design detectors with larger saturation energies, so that the addition of $B_\perp$ will be unnecessary. Greatly improved uniformity of detector performance should follow.

The measured cross-talk between pixels was consistent with the feedback-coil/input-coil model described by de Korte *et al.*[8] In this cross-talk mechanism, the common flux-feedback signal (V_{FB}, see Fig. 2) couples from the feedback coil (M_{FB}) directly to the first-stage-SQUID input coil (M_{in1}), inducing a current in the TES bias loop of each pixel in the column. The result is that a pulse in one pixel is accompanied by a small cross-talk pulse in all other pixels in the column. The observed cross-talk pulses were about 2×10^{-4} times the size of the true pulses in the eight-row system, and caused no measurable degradation of spectrometric performance. Because the strength of the effect depends inversely on the number of rows in the TDM, in a 32-row × 32-column array the cross-talk pulses would be four times smaller. If further reduction of cross-talk were required for a particularly stringent application, various measures could be undertaken, including software correction, injection of a flux signal of the opposite sign during row switches, and increasing the inductance in the TES bias loop.

In summary, we have demonstrated a prototype, 14-pixel, γ-ray microcalorimeter array. The best energy resolution of a single pixel was 25 eV at 103 keV, and the average resolution over the array was 47 eV. Based on the presented results and calculations, we see no obstacles to building a kilopixel array. Future work will focus on improving pixel yield and uniformity and on system engineering for a complete spectrometer.

The authors thank Marcel van den Berg, Caroline Kilbourne, and David Palmer for technical assistance. This work was supported in part by DOE-NNSA, NIST-EEEL Director's Reserve, and the Intelligence Community Postdoctoral Fellowship Program.

[1] M. F. Cunningham, J. N. Ullom, T. Miyazaki, S. E. Labov, J. Clarke, T. M. Lanting, A. T. Lee, P. L. Richards, J. Yoon, and H. Spieler, Appl. Phys. Lett. **81**, 159 (2002).
[2] T. Oshima, Presented at the Third International Workshop on Transition Edge Sensor Device Physics, Gainsville, FL, 2006 (unpublished).
[3] B. L. Zink, J. N. Ullom, J. A. Beall, K. D. Irwin, W. B. Doriese, W. D. Duncan, L. Ferreira, G. C. Hilton, R. D. Horansky, C. D. Reintsema, and L. R. Vale, Appl. Phys. Lett. **89**, 124101 (2006).
[4] J. N. Ullom, W. B. Doriese, G. C. Hilton, J. A. Beall, S. Deiker, W. D. Duncan, L. Ferreira, K. D. Irwin, C. D. Reintsema, and L. R. Vale, Appl. Phys. Lett. **84**, 4206 (2004).
[5] J. N. Ullom, J. A. Beall, W. B. Doriese, W. D. Duncan, L. Ferreira, G. C. Hilton, K. D. Irwin, C. D. Reintsema, and L. R. Vale, Appl. Phys. Lett. **87**, 4103 (2005).
[6] J. A. Chervenak, K. D. Irwin, E. N. Grossman, J. M. Martinis, C. D. Reintsema, and M. E. Huber, Appl. Phys. Lett. **74**, 4043 (1999).
[7] J. Yoon, J. Clarke, J. M. Gildemeister, A. T. Lee, M. J. Myers, P. L. Richards, and J. T. Skidmore, Appl. Phys. Lett. **78**, 371 (2001).
[8] P. A. J. de Korte, J. Beyer, S. Deiker, G. C. Hilton, K. D. Irwin, M. Macintosh, S. W. Nam, C. D. Reintsema, L. R. Vale, and M. E. Huber, Rev. Sci. Instrum. **74**, 3807 (2003).
[9] C. D. Reintsema, J. Beyer, S. W. Nam, S. Deiker, G. C. Hilton, K. D. Irwin, J. M. Martinis, J. N. Ullom, L. R. Vale, and M. Macintosh, Rev. Sci. Instrum. **74**, 4500 (2003).
[10] W. B. Doriese, J. A. Beall, W. D. Duncan, L. Ferreira, G. C. Hilton, K. D. Irwin, C. D. Reintsema, J. N. Ullom, L. R. Vale, and Y. Xu, Nucl. Instrum. Methods Phys. Res. A **559**, 808 (2006).
[11] A. E. Szymkowiak, R. L. Kelley, S. H. Moseley, and C. K. Stahle, J. Low Temp. Phys. **93**, 281 (1993).
[12] J. M. Martinis, G. C. Hilton, K. D. Irwin, and D. A. Wollman, Nucl. Instrum. Methods Phys. Res. A **444**, 23 (2000).